GLOBAL JOURNAL OF ENGINEERING RESEARCH VOL 10, NO. 1&2, 2011: 113-124

 ISSN 1596-292x
www.globaljournalseries.com; Info@globaljournalseries.com

3D STUDY OF BIFACIAL SILICON SOLAR CELL UNDER INTENSE LIGHT CONCENTRATION AND UNDER EXTERNAL CONSTANT MAGNETIC FIELD.

M. ZOUNGRANA, I. ZERBO, A. SERE, B. ZOUMA AND F. ZOUGMORE

(Received 6, July 2011; Revision Accepted 12, Octorber 2011)

ABSTRACT

This work presents a three-dimensional study of bifacial silicon solar cell under intense light concentration and under constant magnetic field. This approach is based on the resolution of the minority continuity equation, taking into account the distribution of the electric field in the bulk evaluated as a function of both majority and minority carrier densities. In this approach, new analytical expressions of diffusion length, diffusion coefficient and excess minority carrier density was established for front illumination. The effect of magnetic field on excess minority carrier generation, carriers mobility, carriers density and electric parameters profile are then analysed.

KEYWORDS 1- Silicon; 2-Light concentration; 3- Magnetic Fields; 4- Diffusion parameters; 5- Electric field.

1. INTRODUCTION

The efficiency of a solar cell is closely bound to its electronics properties mainly governed by the diffusion length, diffusion coefficient and lifetime of electrons and holes. However, some external factors as magnetic field *(Betser et al.,1995), (Serafettin Erel, 2002), (Mamadou et al., 2004),* external electric field *(Coors et al., 1998), (Pelanchon et al., 1992), (Dieng et al., 2009),* intense light *(Pelanchon et al., 1992), (Agroui et al., 2003)* and internal factors as grain size *(Barro et al., 2008)*, grain boundary recombination velocity *(Ba et al., 2003)*, electric field in the bulk due to carrier concentration (*Pelanchon et al., 1992*) can influence the solar cell quality.

In this work, we propose a three dimensional study of bifacial solar cell under intense light concentration (more than 50 suns) and under external variable magnetic field. The calculations were carried out in the case of a polycrystalline device with columnar grain orientation under front side illumination. This approach is based on the resolution of the continuity equation, taking into account the distribution of electric field in the bulk evaluated as a function of both majority and minority carrier densities *(Pelanchon et al., 1992)*. In this approach, new analytical expressions of

M. Zoungrana, Laboratoire des Matériaux et Environnement, Département de Physique, UFR-SEA, Université de Ouagadougou, BURKINA FASO.
I. Zerbo, Laboratoire des Matériaux et Environnement, Département de Physique, UFR-SEA, Université de Ouagadougou, BURKINA FASO.
A. Sere, Département de Physique, Institut des Sciences Exactes et Appliquées, Université Polytechnique de Bobo Dioulasso, BURKINA FASO
B. Zouma, Laboratoire des Matériaux et Environnement, Département de Physique, UFR-SEA, Université de Ouagadougou, BURKINA FASO.
F. Zougmore, Laboratoire des Matériaux et Environnement, Département de Physique, UFR-SEA, Université de Ouagadougou, BURKINA FASO.

recombination and electric parameters, excess minority carrier density was established for front side illumination. The effects of magnetic field on diffusion length, diffusion coefficient and excess minority carrier generation and profile are then analysed.

2. MODEL AND ASSUMPTION

2.1 Analytical formulation

We consider a bifacial polycrystalline Si-solar cell operating under a concentrated multispectral light. This kind of solar cell, because of its manufacture technique is constituted of several grains of different sizes and forms separated by grain boundaries, whom are very great recombination centers. Macroscopic and microscopic parameters of the solar cell are deeply dependent on grain boundaries. These grain boundaries are either grains junctions or either local distortions caused by solar cell manufacture foulness.

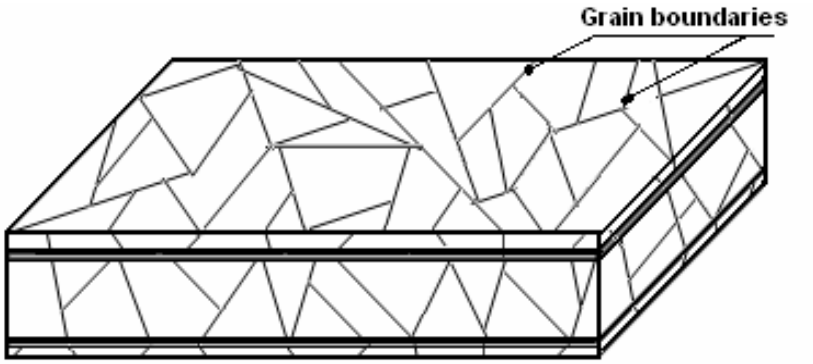

Figure 1: Grains and grains boundaries illustration

With no loss in generality, we consider a columnar model in where the solar cell is modelled as a regular array of parallelepipedic grains connected in parallel (Dugas J, 1994).

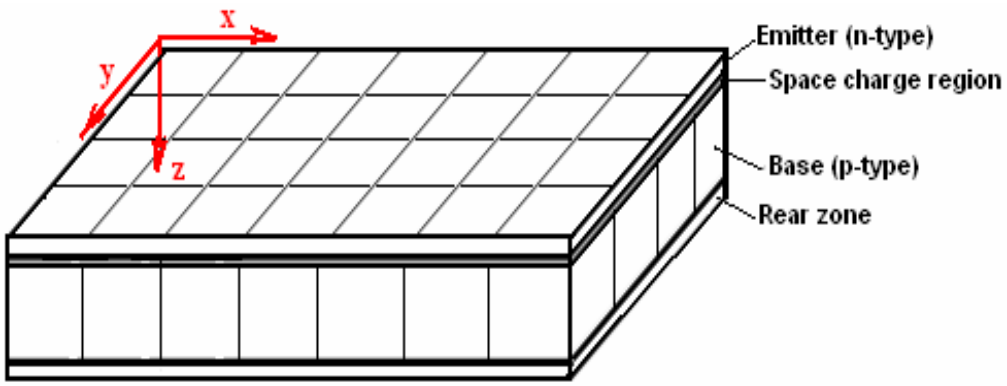

Figure 2: Columnar model assumption

Each grain has a square section (g_x = g_y) and a thickness *H* as shown in Figure 3.

The recombination planes are assumed to be thin surfaces between two adjacent grains and are located at $x = \pm \frac{g_x}{2}$ and $y = \pm \frac{g_y}{2}$, respectively perpendicular to the x- and y-axis of a cartesian coordinates (O; x; y; z) *(Ba et al, 2003)*. The grain boundaries are perpendicular to the junction and their effective recombination velocity S_{gb} is constant.

The cell is excited uniformly on the emitter surface by an intense light concentration (more than 50 suns). The light penetrates the junction at the plane *z = 0* and the back surface is

situated at *z = H*. Because of the light intensity, carrier concentration in the base is not uniform. So, we take into account the electric field *E(z)* due to the difference of carrier concentration on *z* axis *(Pelanchon et al., 1992)*.

To investigate the magnetic field influence on carrier behaviour and photocurrent, we applied a variable external magnetic field with the induction *B* parallel to the surface of the n-p junction.

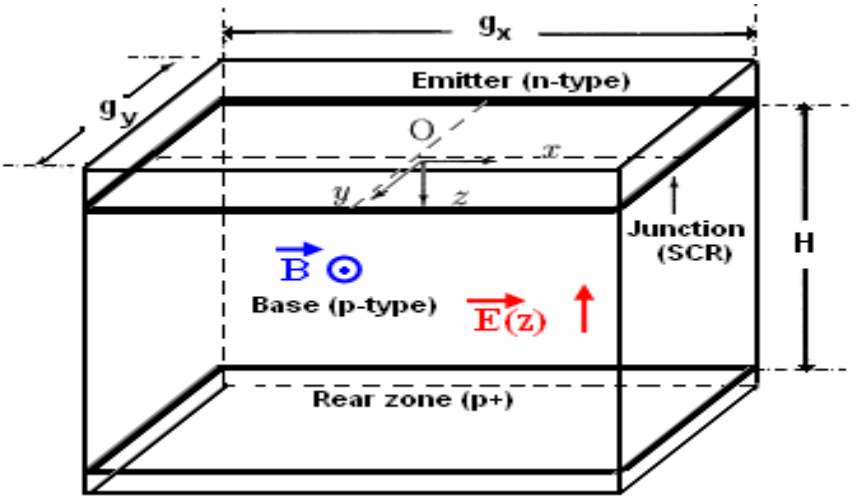

Figure 3: Theoretical model of square grain with an external magnetic field and internal electric field.

If we take into account the electric field *E(z)* in the base, his expression on z axis is given by equation 1 below *(Pelanchon et al., 1992)*:

$$E(z) = \frac{D_p - D_n}{\mu_p + \mu_n} \cdot \frac{1}{\delta_n(x,y,z)} \frac{\partial \delta_n(x,y,z)}{\partial z} \quad (1)$$

Introducing this expression of the electric field in the model of *figure 3* and taking into account our assumptions, the expression of excess minority carriers distribution in the solar cell is:

$$\frac{\partial \delta(x,y,z)}{\partial t} = \frac{1}{e}\vec{\nabla}.\overrightarrow{J_n} + G(z) - R(z) \quad (2)$$

$G(z)$ is the excess minority carrier generation at position z , and *R(z)* the recombination rate at this position: for front side illumination *(Mohammad S N, 1987), (Touré et al., 2010)*, $G(z) = C \cdot \sum_{i=1}^{3} a_i \cdot e^{-b_i z}$

a_i and b_i are deduced from modelling of the generation rate considered for over all the solar radiation spectrum *(Samb et al., 2009).*

Recombination rate expression is $R(z) = \frac{\delta_n(x,y,z)}{\tau_n}$ where τ_n is electron lifetime in the base, and $\delta_n(x,y,z)$ the excess minority carrier density in the base of our illuminated solar cell. The expression of $\overrightarrow{J_n}$ is given by the equation of transportation phenomenon *(Betser et al., 1995)*:

$$\overrightarrow{J_n} = \overrightarrow{J_d} + \overrightarrow{J_{In}} + \overrightarrow{J_c} = e.D_n.\vec{\nabla}\delta(x,y,z) - \mu_n.\overrightarrow{J_n}\Lambda\vec{B} + e.\mu_n.\delta.(x,y,z).\vec{E} \quad (3)$$

In this expression:

$\overrightarrow{J_d}$ represents carriers diffusion current on *x,y,z* axis, $\overrightarrow{J_{In}}$ represents the *y* axis magnetic field induced current and $\overrightarrow{J_c}$ represents conduction current on *z* axis, with $\vec{B} = B\vec{j}, \quad B(x) = B(z) = 0$ $\vec{E} = -E(z)\vec{k}$.

When the solar cell rear side is illuminated, we suppose a uniform carrier distribution along *x and y* axis at any base depth. Therefore, conduction current doesn't exist according to these axes, so that: $\frac{\partial J_c}{\partial x} = \frac{\partial J_c}{\partial y} = 0$

On the basis of these assumptions, we deduce the expressions of electrons density current $\overrightarrow{J_n}$ and the components of $\vec{\nabla}.\overrightarrow{J_n}$. Taking into account the coordinates of $\overrightarrow{J_n}$, equation 2 can be written in permanent regime $(\frac{\partial \delta(x,y,z)}{\partial t} = 0)$ as:

$$C_x \cdot \frac{\partial^2 \delta(x,y,z)}{\partial x^2} + C_y \cdot \frac{\partial^2 \delta(x,y,z)}{\partial y^2} + \frac{\partial^2 \delta(x,y,z)}{\partial z^2} + \frac{G(z)}{D^*} - \frac{\delta(x,y,z)}{L^{*2}} = 0 \qquad (4)$$

with $C_x = \frac{D_n(\mu_p + \mu_n)}{2.D_n.\mu_n + D_n.\mu_p - \mu_n.D_p}$, $C_y = \frac{D_n(\mu_p + \mu_n).(1 + \mu_n^2 B^2)}{2.D_n.\mu_n + D_n.\mu_p - \mu_n.D_p}$ and

$D^* = \frac{(D_n - \mu_n.A)}{1 + \mu_n^2 \cdot B^2}, L^{*2} = \tau_n \cdot D^*$ with $A = \frac{D_p - D_n}{\mu_p + \mu_n}$ and $R(z) = \frac{\delta(x,y,z)}{\tau_n}$

Equation 4 is the continuity equation of a solar cell under constant multispectral illumination and without magnetic field. Our model leads us to news expressions of carrier diffusion length (L^*) and carrier diffusion coefficient (D^*), which depend on magnetic field, electrons and holes mobility, and diffusion coefficients (D_p, D_n). In these expressions, the coefficient $A = \frac{D_p - D_n}{\mu_p + \mu_n}$ characterizes the approximation made on the electric field and $C_m = 1 + \mu_n^2 \cdot B^2$ the one made on the magnetic field.

We present on the following table, the values of diffusion parameters in our model for null value of magnetic field, comparatively to the literature values (Equer Bernard, 1993).

	Diff length	Diff coefficient
Literature values	L_n=0.02 cm	D_n=26 cm².s-¹
Front illumination	L^*=0.027 cm	D^*=45.8 cm².s-¹

Table 1: Comparative table values of electron diffusion parameters

We note that for a front illumination, diffusion parameters values increase when taking into account excess minority carrier gradient concentration electric field. It appears that electric field application reduces the traps, and permits to the carriers to flow easily and to browse a bigger distance before recombining.

Figures 4 and 5 give the carriers diffusion length (L^*) and carriers diffusion coefficient (D^*) profiles versus magnetic field.

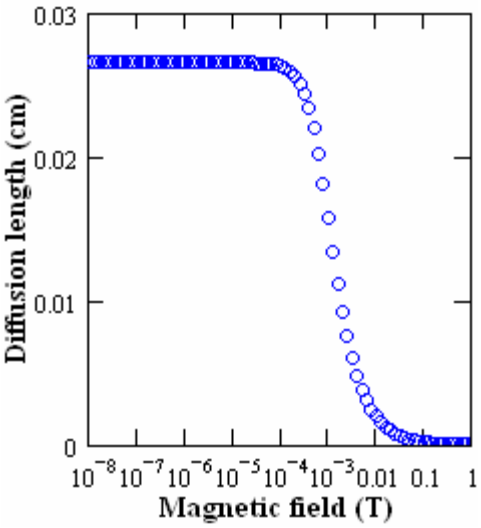

Figure 4: Diffusion length

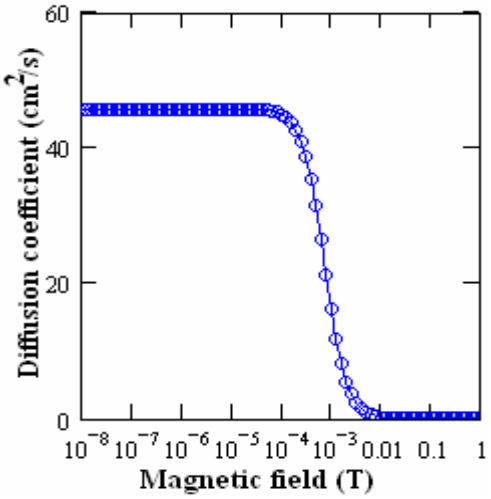

Figure 5: Diffusion coefficient

Figure 4 and 5: Effect of magnetic field on Diffusion length and Diffusion coefficient

Figure 4 and 5 show that diffusion length and diffusion constant decrease with magnetic field increase. These figures also show that for very low magnetic field (7.10^{-5} T), diffusion length and carriers diffusion coefficients are not magnetic field dependent. On the other hand, for values of magnetic field between 7.10^{-5} T and 0.12 T, carriers diffusion lengths and carriers diffusion coefficients values decreases before annulling themselves around 0.12 T. This behaviour is the consequence of Hall effect, which modifies electrons trajectories. One also notes that the order of the terrestrial magnetic field (5.10^{-5} T) doesn't have an effect on carrier diffusion length and carrier diffusion coefficient values, because they are situated on the tray ($B < 7.10^{-5}$ T).

2.2. Solution of the continuity equation

Equations 4 is a partial derivative differential equation for which the general shape of the solution can be written *(Ducas J, 1994)* as:

$$\delta(x,y,z) = \sum_j \sum_k Z_{j,k}(z) \cdot \cos(C_{xj}x) \cdot \cos(C_{yk}y), \quad \text{with} \quad C_{xj} = \frac{C_j}{C_x} \quad \text{and} \quad C_{yk} = \frac{C_k}{C_y} \qquad (5)$$

The coefficients C_j and C_k are determinated by the boundary conditions on the grain boundaries for $x = \pm\frac{g_x}{2}$ and $y = \pm\frac{g_y}{2}$ respectively:

$$\left[\frac{\partial\delta(x,y,z)}{\partial x}\right]_{x=\pm\frac{g_x}{2}} = \pm\frac{Sgb}{D^*} \cdot \delta(\pm\frac{g_x}{2}, y, z) \quad and \quad \left[\frac{\partial\delta(x,y,z)}{\partial y}\right]_{y=\pm\frac{g_y}{2}} = \pm\frac{Sgb}{D^*} \cdot \delta(x, \pm\frac{g_y}{2}, z) \qquad (6)$$

The coefficients C_{xj} and C_{yk} are given by the transcendental equations:

$$C_{xj} \tan(C_{xj} \cdot \frac{g_x}{2}) = \frac{Sgb}{D^*} \quad and \quad C_{yk} \tan(C_{yk} \cdot \frac{g_y}{2}) = \frac{Sgb}{D^*} \qquad (7)$$

While taking into account that $\cos(C_{xj}x)$ and $\cos(C_{yk}y)$ are orthogonal functions, the z dependence of $\delta(x,y,z)$ can be expressed for a front side illumination as:

$$Z_{jk}(z) = A_{jk}\cosh\left(\frac{z}{L_{j,k}}\right) + B_{jk}\sinh\left(\frac{z}{L_{j,k}}\right) - \sum_{i=1}^{3} K_i e^{-bi\cdot z} \quad (8)$$

with:

$$\frac{1}{L_{j,k}} = \left[C_j^2 + C_k^2 + \frac{1}{L_n^2}\right]^{\frac{1}{2}} \quad and \quad \frac{1}{D_{j,k}} = \frac{16\cdot\sin(C_{xj}\cdot\frac{g_x}{2})\cdot\sin(C_{yk}\cdot\frac{g_y}{2})}{D^*\cdot\left[\sin(C_{xj}\cdot g_x)+C_{xj}\cdot g_x\right]\cdot\left[\sin(C_{yk}\cdot g_y)+C_{yk}\cdot g_y\right]}$$

The expressions of the coefficients A_{jk} and B_{jk} are obtained by solving *equation 5*, with the following boundary conditions at the two edges of the base region *(Diallo et al., 2006), (Zouma et al., 2009)*:

- the junction interface at $z=0$: $S_f = \frac{D^*}{\delta(x,y,0)}\cdot\left[\frac{\partial\delta(x,y,z)}{\partial z}\right]_{z=0}$

- the rear side at $z=H$: $S_b = -\frac{D^*}{\delta(x,y,H)}\cdot\left[\frac{\partial\delta(x,y,z)}{\partial z}\right]_{z=H}$

This lead to:

$$A_{jk} = \sum_{i=1}^{3} K_i \cdot \frac{\frac{1}{L_{j,k}}\cdot\left(\frac{S_f}{D^*}-bi\right)\cdot\exp(-bi\cdot H)+\beta_{j,k}\cdot\left(\frac{S_f}{D^*}+bi\right)}{\frac{S_f}{D^*}\cdot\beta_{j,k}+\frac{1}{L_{j,k}}\cdot\alpha_{j,k}} \quad (9)$$

and

$$B_{jk} = \sum_{i=1}^{3} K_i \cdot \frac{\left[\frac{S_f}{D^*}\cdot\left(\frac{S_b}{D^*}-bi\right)\cdot\exp(-bi\cdot H)-\alpha_{j,k}\cdot\left(\frac{S_f}{D^*}+bi\right)\right]}{\frac{S_f}{D^*}\cdot\beta_{j,k}+\frac{1}{L_{j,k}}\cdot\alpha_{j,k}}$$

with

$$\alpha_{j,k} = \frac{1}{L_{j,k}}\cdot\sinh\left(\frac{H}{L_{j,k}}\right) + \frac{S_b}{D^*}\cdot\cosh\left(\frac{H}{L_{j,k}}\right) \quad and$$

$$\beta_{j,k} = \frac{1}{L_{j,k}}\cdot\cosh\left(\frac{H}{L_{j,k}}\right) + \frac{S_b}{D^*}\cdot\sinh\left(\frac{H}{L_{j,k}}\right)$$

3. SIMULATION RESULTS AND DISCUSSIONS

We present in this part a 3-D study of magnetic field effects, on the excess minority carriers generation and recombination parameters in the bulk of the base of a bifacial solar cell illuminated by his front side.

This study in modelling is made on the basis of the following parameters: base depth: H = 300 μm; doping level: $N_A = 10^{16}\,cm^{-3}$; electron diffusion length: $L_n = 200\mu m$; electrons diffusion coefficient: $D_n = 26cm^2.s^{-1}$; holes diffusion coefficient: $D_p = 4cm^2.s^{-1}$; electron mobility: $\mu_n = 1350cm.s^{-1}$; hole mobility: $\mu_p = 150cm.s^{-1}$.

3.1. Effect of magnetic field and back-surface recombination velocity on excess minority carrier density

We show on Figure 6, magnetic field and back surface recombination velocity influences on excess minority carrier photogeneration in the region close to the junction ((z= 0.0001 cm).

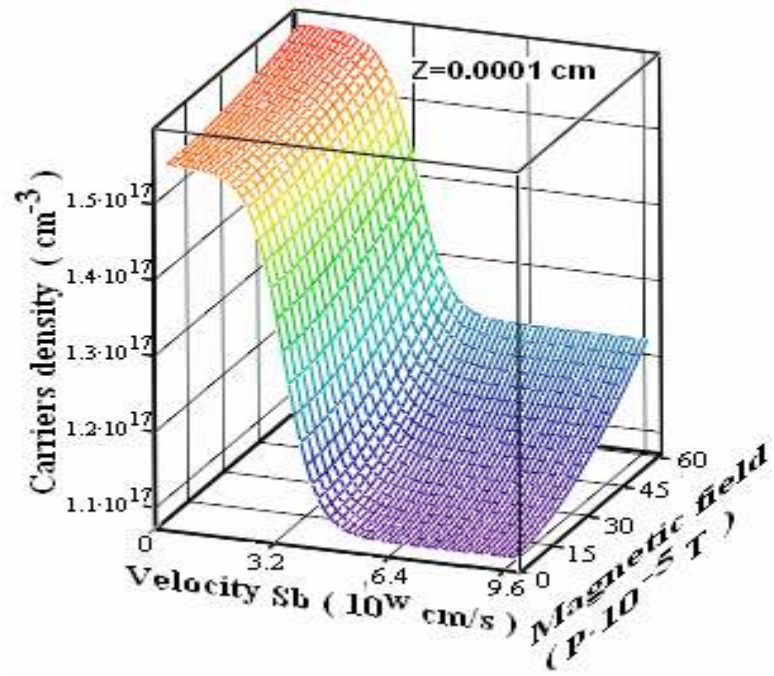

Figure 6: Excess minority carriers profile in the base of a photoexcited cell versus back surface recombination velocity and magnetic field: C=200 suns; z=0.0001cm; $g_x=g_y=3.10^{-3}$cm; $S_f=10^1$ cm.s^{-1}; Sgb=10^2 cm.s^{-1}.

We notice on this figure that for a front side illumination, the density of the carriers photogenerated close to the junction decreases with the increase of the back surface recombination velocity and increase with magnetic field increasing. For a front side illumination, the maximal quantity of carrier photogenerated close to the junction is observed if the two following conditions are simultaneously verified: small values of back surface recombination velocity and big values of the magnetic field.

We also observe that the increase of carrier density close to the junction with the magnetic field is more important at the big values of back surface recombination velocity. This result is bound to the decrease of the back surface recombination velocity with the magnetic field increase *(Samb et al., 2010)*. Electrons quantity in the region close to the junction increase phenomenon with the magnetic field increases will have a very big influence on the photocurrent and the photovoltage. Indeed, photocurrent and photovoltage being bound closely to the quantity of carriers that crosses the junction, the effects of magnetic field for a front side illumination will have a big influence on them.

3.2. Effect of magnetic field and grain size on excess minority carrier density

The following curves put in evidence magnetic field influence on excess minority carrier photogeneration in the bulk of the base for front illumination.

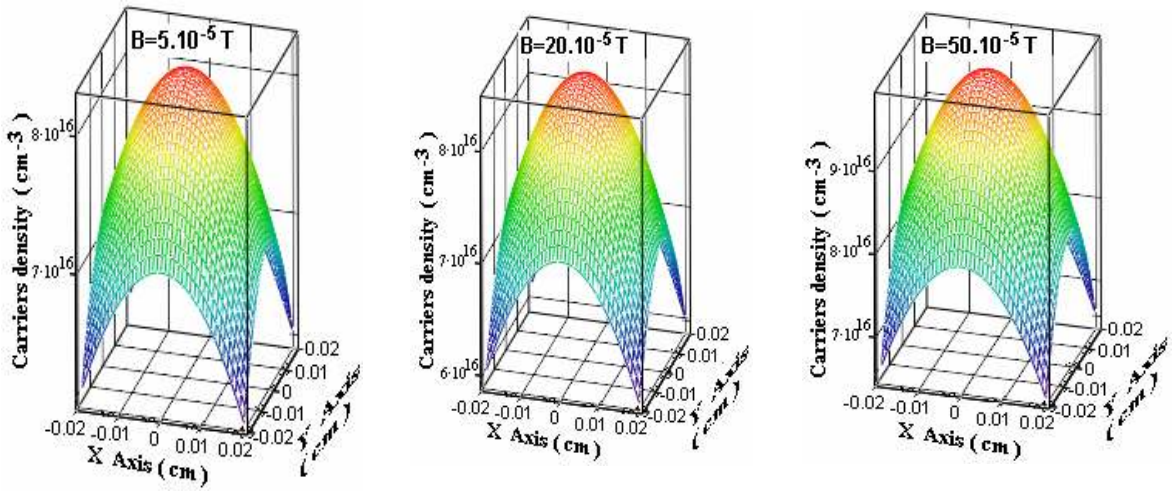

Figure 7: Excess minority carriers profile in the base of a front photoexcited cell in versus grain width (X×Y) and magnetic field for: C = 200 suns; z = 0.0001 cm; S_f=10¹cm.s⁻¹; S_b = 10^4 cm.s⁻¹; Sgb = 10² cm.s⁻¹

We show on Figure 7 the effect of tree applied values of magnetic field ($B = 5.10^{-5} T$, $B = 20.10^{-5} T$, $B = 50.10^{-5} T$) on the excess minority carriers near the junction (z=0.0001cm) for a front illumination. We notice globally that an increase of the applied magnetic field lead to a very sensitive increase of the excess minority carrier photogenerated in the base. This very logical report is the consequence of Hall effect. This result perfectly agrees with diffusion length and carrier diffusion coefficient decrease with magnetic field increase because of Hall effect on carrier mobility. It characterizes also a tendency of junction crossing excess minority carrier quantity reduction

3.3. Effect of magnetic field and base depth on excess minority carrier density

In this paragraph, we study the minority carrier density profiles for a front illumination mode and with respect to magnetic field and light intensity. We get in the situation where a part of photogenereted carrier in the base of the solar cell crosses the junction to participate to the photocurrent. For that, we work with a junction recombination velocity $S_f = 10^4 cm.s^{-1}$ and back surface recombination velocity $S_b = 10^3 cm.s^{-1}$.

We show on Figure 8, excess minority carrier density profiles for front illuminations and with respect to base depth and magnetic field.

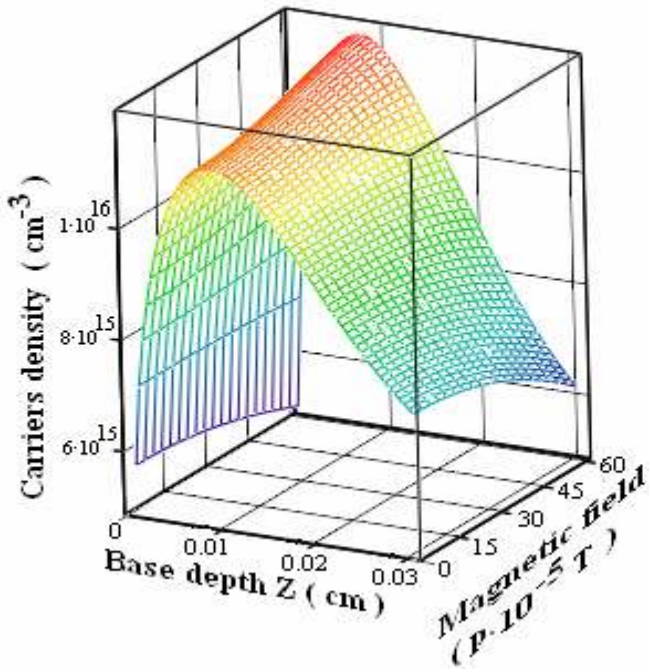

Figure 8: Excess minority carriers profile in the base of a photoexcited cell versus base depth and magnetic field: C=200 suns; $g_x=g_y=3.10^{-3}$cm; $S_f=10^4$ cm.s^{-1}; $S_b=10^3$ cm.s^{-1}; Sgb=100 cm.s^{-1}.

Figure 8 shows the effect of magnetic field on the excess minority carrier density profile in the bulk of the base region for a bifacial solar cell front illuminated. The observed curves exhibit two characteristics regions in the base.

The first region closed to the junction with a positive slope which increases when magnetic field increase. The maximum of carrier density increases with respect to magnetic field and becomes more and more closed to the junction and we deduce that the magnetic field increases carrier concentration in this region. The maximum of carriers density increasing is a consequence of the Hall effect because of the external magnetic field. This region corresponds to minority carrier collection region. Indeed, Hall effect entails a deviation of electrons trajectories and imposes them a bigger distance to browse with a higher recombination probability before reaching the junction. The displacement of the maxima of carrier density toward the junction is discerned like a reduction of the space-charge region comparatively to the initial diffusion depletion layer *(Sissoko et al, 1998)*.

The second region with a negative slope corresponds to minority carrier recombination region. Indeed, the carriers created in this region of the base don't have enough energy to surmount the traps and to go back up the slope to participate to current production.

We also notice that excess minority carrier concentration decrease with respect to magnetic field in the base rear zone. This behaviour is the consequence of back surface recombination velocity to which solar cell rear zone is strongly exposed.

3.4. Effect of magnetic field on excess minority carrier density in Short circuit and open circuit situation

In Figure 9 and 10 are displayed the base excess minority carrier density profiles in *x*- and *z*- axis and with respect to magnetic field in short - and open- circuit conditions. The solar cell is illuminated with an intense light (> 50 suns).

For different magnetic field values, it is observed that carrier generation in every position of base depth is uniform, even it decreases when approaching the grain boundary whose activity is described by in an infinite value grain boundary recombination velocity ($S_{gb} = \infty$).

We observe on figure 9 that for a front side illumination, carriers density profile according to base depth in short circuit situation present the same behaviour that the one of *figure 8*: positive slope in region close the junction, null slope (curves maxima) and negative slope in base inside. However, we observe that it appears a fourth region in rear zone, where carriers increase slightly with base depth. This phenomenon that had not appeared on *figure 8,* is more accentuated for the big values of the magnetic field ($B = 80.10^{-5} T$). This fourth zone appearance is probably the consequence of back surface recombination decrease with respect to magnetic field increase.

One also notes that for magnetic field big values, carrier densities curves peaks increases and move back toward the junction. These two behaviours that appear in *short circuit* confirm carriers accumulation in the region close to the junction and carriers diffusion phenomena decrease with respect to magnetic field increase.

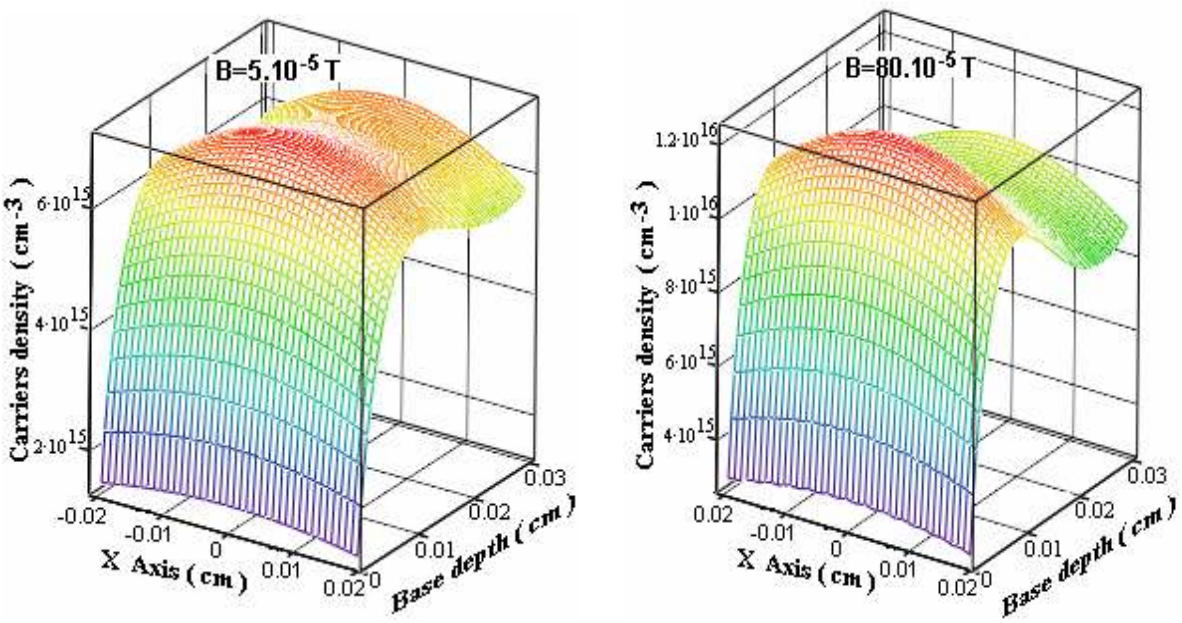

Short circuit

Figure 9: Magnetic field effect on excess minority carriers profile in x- and z- axis in short circuit situation: S_f=10⁸ cm.s⁻¹, S_b=10³cm.s⁻¹, Sgb=10²cm.s⁻¹, C=200 suns.

We observe on *figure 10* that for a front side illumination, carriers density profiles according to base depth in open circuit situation present negative slopes for every value of magnetic field.

This report is the consequence of solar cell working order. Indeed, in open circuit situation, junction recombination velocity is hopeless and the carriers don't cross the junction. We notice here also that carriers densities values are raised more at magnetic field big values for the above evoked reasons.

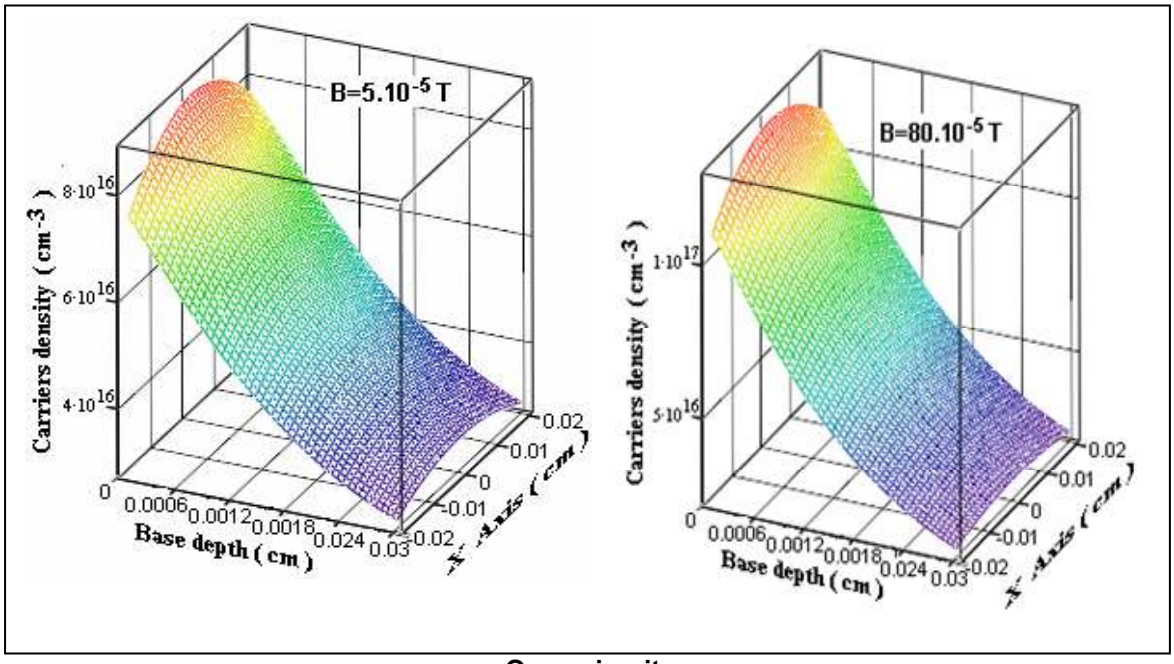

Open circuit

Figure 10: Magnetic field effect on excess minority carriers profile in x- and z- axis in open circuit situation: S_f=10¹cm.s⁻¹, S_b=10³cm.s⁻¹, Sgb=10²cm.s⁻¹,C=200 suns.

4. CONCLUSION

The hold in account of electric field due to carriers concentration in the bulk and the magnetic field lead us to a new shape of continuity equation, diffusion length and carrier diffusion coefficient which are function of both magnetic field, electrons and holes mobility, and their diffusions constants (D_n, D_p). The curves of carrier diffusion length and carrier diffusion coefficient decrease with magnetic field increase. We also observed that the hold in account of carrier gradient concentration electric field (in intense light concentration mode) increase these coefficients values under the non approximated electric field ones.

With regard to magnetic field, it is observed that it has a big influence on carriers generation. The limiting effects of magnetic field on carrier diffusion length (L^*), carrier diffusion coefficient (D^*) and excess minority carrier density ($\delta(x,y,z)$) are pronounced for magnetic field values greater than $7.10^{-5}T$ ($B > 7.10^{-5}$ T).

We also observe that the magnetic field has a big influence on electrons behaviour of solar cell working different states: short circuit, open circuit and normal situation working. Indeed in any case, the magnetic field increases carrier presence in the region close to the junction. It appears therefore that the magnetic field reinforces solar cell Back Surface Field (BSF) while reducing the recombination in rear zone and the traps in the volume of the basis. Paradoxically, the quantity of carriers that cross the junction decreases with magnetic field increase. This paradox brings us to conclude a possible electrons blockage in the region close to the junction with magnetic field increase. This behaviour is the consequence of Hall effect, which modifies electrons trajectories *(Vardanyan et al., 1998).*

REFERENCES

Agroui, K., Belghachi, A and et Kadri, S., 2003. Rev. Energ. Ren.: IPWE (2003) 19-25.

Ba, B., Kane, M and Sarr, J., 2003. Solar Energy Materials & Solar Cells 80: 143-154.

Barro, F. I., Mbodji, S., Ndiaye, M., Ba, E and Sissoko, G., 2008. Proceedings of 23rd European Photovoltaic Solar Energy Conference.

Betser, Y., Ritter, D., Bahir, G., Cohen, S and

Sperling, J., 1995. App. Phys. Lett. 67, (13): 1883-1884.

Coors, S., Schneider, B and Bohm, M., 1998. 2nd World conference and exhibition on photovoltaic solar energy conversion.

Diallo, H. L., Ly, I., Zoungrana, M., Nzonzolo., Barro, F. I and Sissoko, G., 2006. 21st European Photovoltaic Solar Energy Conference.

Dieng, A., Sow, M. L., Mbodji, S., Samb, M. L., Ndiaye, M., Thiame, M., Barro, F. I and Sissoko, G., 2009. Proceedings of 24th European Photovoltaic Solar Energy Conference.

Dugas, J., 1994. Solar Energy Materials and Sollar cells, 32: 71-88.

Equer, B., 1993. Ellipses, Energie solaire photovoltaïque, 1,

Mohammad, S. N., 1987. Journal of Applied Physics, 61, (2): 767 – 772.

Pelanchon, F., Sudre, C and Moreau, Y., 1992. 11th European Photovoltaic Solar Energy Conference.

Samb, M. L., Dieng, M., Mbodji, M., Mbow, N., Thiam, N., Barro, F, I and Sissoko, G., 2009. Proceedings of 24th European Photovoltaic Solar Energy Conference.

Samb, M. L., Zoungrana, M., Sam, R., Dione, M. M., Deme. M. M and Sissoko, G., 2010. Journal des Sciences 10, (4): 23-38.

Serafettin Erel., 2002. Solar Energy Materials & Solar Cells, 71: 273-280.

Sissoko, G., Dieng, B., Corréa, A., Adj, M and Azilinon, A., 1998. World Renewable Energy Congress.

Touré, F., Zoungrana, M., Sam, R., Diop, M. T. D., Barro, F. I and Sissoko, G., 2010. Journal des Sciences 10, (4): 16-22.

Vardanyan, R. R., Kerst, U., Wawer, P and Wagemann, H, 1998. Proceeding of 2nd World conference and exhibition on photovoltaic solar energy conversion.

Zouma, B., Maïga, A. S., Dieng, M., Zougmaré, F and Sissoko, G., 2009. Global Journal of Pure and Applied Sciences, 15, (1): 117-124.